

2002

Collisional and Radiative Processes in High-Pressure Discharge Plasmas

Kurt H. Becker

Peter F. Kurunczi

Karl H. Schoenbach
Old Dominion University

Follow this and additional works at: https://digitalcommons.odu.edu/bioelectrics_pubs

Part of the [Plasma and Beam Physics Commons](#)

Repository Citation

Becker, Kurt H.; Kurunczi, Peter F.; and Schoenbach, Karl H., "Collisional and Radiative Processes in High-Pressure Discharge Plasmas" (2002). *Bioelectrics Publications*. 243.
https://digitalcommons.odu.edu/bioelectrics_pubs/243

Original Publication Citation

Becker, K. H., Kurunczi, P. F., & Schoenbach, K. H. (2002). Collisional and radiative processes in high-pressure discharge plasmas. *Physics of Plasmas*, 9(5), 2399-2404. doi:10.1063/1.1449464

Collisional and radiative processes in high-pressure discharge plasmas^{a)}

Kurt H. Becker^{b)} and Peter F. Kurunczi^{c)}

Department of Physics, Stevens Institute of Technology, Hoboken, New Jersey 07030

Karl H. Schoenbach

Physical Electronics Research Institute, Old Dominion University, Norfolk, Virginia 23529

(Received 30 October 2001; accepted 26 November 2001)

Discharge plasmas at high pressures (up to and exceeding atmospheric pressure), where single collision conditions no longer prevail, provide a fertile environment for the experimental study of collisions and radiative processes dominated by (i) step-wise processes, i.e., the excitation of an already excited atomic/molecular state and by (ii) three-body collisions leading, for instance, to the formation of excimers. The dominance of collisional and radiative processes beyond binary collisions involving ground-state atoms and molecules in such environments allows for many interesting applications of high-pressure plasmas such as high power lasers, opening switches, novel plasma processing applications and sputtering, absorbers and reflectors for electromagnetic waves, remediation of pollutants and waste streams, and excimer lamps and other noncoherent vacuum-ultraviolet light sources. Here recent progress is summarized in the use of hollow cathode discharge devices with hole dimensions in the range 0.1–0.5 mm for the generation of vacuum-ultraviolet light. © 2002 American Institute of Physics. [DOI: 10.1063/1.1449464]

I. INTRODUCTION

Hollow cathode discharge devices with hole dimensions in the cathode in the range from 0.1–0.5 mm (microhollow cathode discharges or MHCDs) can be operated at high pressure (up to and exceeding atmospheric pressure). MHCDs are known to be efficient sources of noncoherent ultraviolet (UV) and vacuum ultraviolet (VUV) radiation when operated in rare gases, rare gas–halide mixtures, and gas mixtures containing rare gases and trace amounts of gases such as H₂, O₂, and N₂. Internal efficiencies in direct current MHCD excimer sources of close to 10% were obtained in Xe at a pressure of about 400 Torr. By applying nanosecond electrical pulses to the dc discharge the efficiency could be increased to approximately 20%. The radiative emittance, which for dc discharges in Xe was measured as 1.4 W/cm², could be increased to over 15 W/cm² through pulsed operation. In addition to rare gas and rare gas halide excimer emission, intense, monochromatic atomic line emissions have been reported from high-pressure MHCD plasmas in rare gases admixed with trace amounts (less than 1%) of H₂, O₂, and N₂. The atomic line emission is the result of a near-resonant energy transfer process involving the excimers and the diatomic molecules. For instance, Ne₂^{*} excimers in the bound ³Σ_u state have enough energy to dissociate H₂ and excite one of the H atoms to the *n*=2 state. The subsequent decay of the excited H atom results in the emission of the 121.6 nm H Lyman-α line. We discuss the results of dc and time-resolved emission spectroscopy in the UV and VUV to elucidate the microscopic mechanisms of the rare gas exci-

mer formation and emission processes, the properties of the MHCD plasma, and microscopic details of the near-resonant energy transfer processes that lead to the emission of the intense atomic line radiation in the range 100–130 nm.

High-pressure MHCD plasma operation exploits the inverse scaling of the hole diameter in a hollow cathode (HC) discharge device with the operating pressure^{1,2} which makes atmospheric-pressure operation possible, if the hole diameter is of the order of about 0.1–0.5 mm. A HC discharge is created by applying an external dc or a time-varying voltage to the electrodes thus forming a potential trough in the cathode cavity and confining the negative glow of the discharge. This results in a strong acceleration of the electrons and a possible oscillatory motion (pendulum electrons).^{3–6} The trapped “pendulum electrons” can undergo many ionizing collisions with the background gas thus creating a high-density plasma which emits intense radiation and is characterized by a very high current density (hollow cathode effect). Figure 1 shows a line-of-sight photograph of the light emission from a MHCD plasma in Xe.

In this paper recent progress in the use of high pressure MHCD plasmas for the generation of noncoherent UV and VUV light is summarized. Spectroscopic studies of the emissions of MHCD plasmas in rare gases, rare gas–halide mixtures, and rare gas mixtures with O₂, H₂, and N₂ following direct current and pulsed excitation of the MHCD device have been carried out in an effort to elucidate the collisional and radiative processes in MHCD plasmas.

II. BACKGROUND

Schoenbach and co-workers were the first to report excimer emissions from MHCD plasmas in Xe and Ar.^{1,2,7–9} Subsequently, excimer emissions were reported from MHCD

^{a)}Paper F12 5, Bull. Am. Phys. Soc. **46**, 100 (2001).

^{b)}Invited speaker. Corresponding author. Electronic mail: kbecker@stevens-tech.edu

^{c)}Present address: Plasmion Corp., Hoboken, New Jersey 07030.

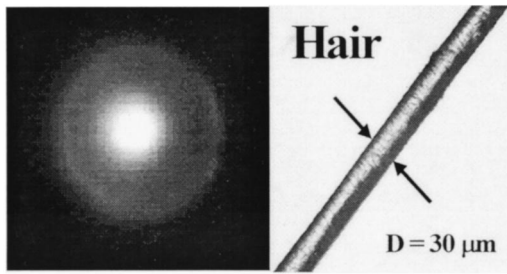
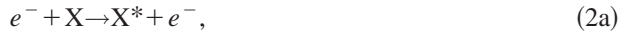


FIG. 1. Line of sight photograph of the emissions from MHCD plasma in Xe at 400 Torr. A human hair with a diameter of $30\ \mu\text{m}$ is shown to illustrate the dimensions of the MHCD device.

plasmas in Ne and He.^{10,11} The most common routes to rare gas excimer formation are either via electron-impact ionization,



where $X = \text{He, Ne, Ar, Kr, or Xe}$ and the asterisk denotes a metastable rare gas atom, or alternatively directly via excitation of metastable rare gas atoms by electrons,



In both cases, the excimer molecules are formed in three-body collisions involving a metastable rare gas atom and two ground-state atoms. Efficient excimer formation requires (i) a sufficiently large number of electrons with energies above the threshold for the metastable formation (or ionization), and (ii) a pressure that is high enough to have a sufficiently

high rate of three-body collisions. Minimum electron energies required for excimer formation range from 11–14 eV in Xe to 20–24 eV in He.

Rare gas excimer emission spectra are dominated by the so-called second continuum which corresponds to a transition from the lowest lying bound $^3\Sigma_u$ excimer state to the repulsive ground state^{12,13} with peak emissions at 170 nm (Xe), 145 nm (Kr), 130 nm (Ar), 84 nm (Ne), and 75 nm (He). The so-called first excimer continua in the rare gases are observed on the short-wavelength side of the second continua and are due to the radiative decay of vibrationally excited levels of the $^1\Sigma_u$ excimer state.

Becker and co-workers¹⁰ reported the emission of intense H Lyman- α emissions from MHCD plasmas in gas mixtures of high-pressure Ne with trace amounts of H_2 . These authors monitored simultaneously the Ne_2^* excimer emission and the Lyman- α emission and observed a dramatic decline in the Ne_2^* excimer emission when H_2 was added to the gas mixture. This provided direct experimental evidence that the near-resonant energy transfer reaction involving Ne_2^* excimers and H_2 molecules is the source of this intense atomic H emission. Earlier, Wieser *et al.*¹⁴ had observed a similar emission of intense, monochromatic H Lyman- α radiation from high-pressure gas mixtures of Ne with trace amounts of H_2 bombarded by high energy electrons and ions and first suggested the above near-resonant energy transfer process as the most likely mechanism leading to the emission of the H Lyman- α line¹⁴ on the basis of spectroscopic studies of the Lyman- α emission.

III. EXPERIMENTAL DETAILS

The electrodes of the MHCD devices used in the present experiments (Fig. 2) are made of 0.1 mm thick molybdenum foils separated by a 0.25 mm insulating spacer with a hole of typically 0.1–0.2 mm diameter in the cathode, the dielectric,

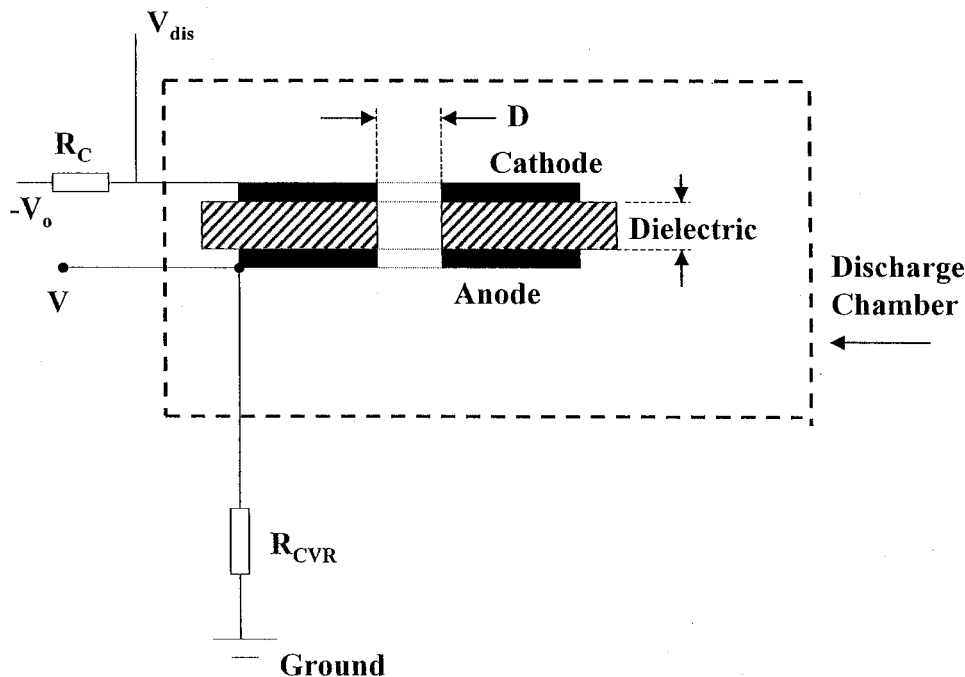


FIG. 2. Schematic diagram of a MHCD device and the circuit diagram for dc operation. The dashed box denotes the boundaries of the discharge chamber.

and in the anode. For dc operation, supply voltages V_0 are typically 400 to 700 V and sustaining (discharge) voltages $V_{\text{Dis}} - R_{\text{CVR}} \cdot I_{\text{Dis}}$ are in the range of 150–300 V depending on the gas pressure and the actual geometry of the MHCD. Discharge currents I_{Dis} vary between 1–10 mA. The circuit includes a resistor R_{CVR} which allows us to monitor the discharge current directly on an oscilloscope along with the discharge sustaining voltage. We can also operate the MHCD in a pulsed dc mode with frequencies up to tens of kHz, pulse lengths from 10 ns to 1 ms and variable pulse separation and duty cycle using a versatile pulse generator. Other modes of excitation include ac excitation with frequencies from a few kHz to several hundred kHz and rf excitation.

Spectral measurements in the range from 120 nm to 400 nm were performed using a 0.5 m scanning monochromator with a grating of 600 G/mm blazed at 150 nm. The discharge chamber with a MgF_2 window was mounted directly to the entrance slit of the monochromator. The spectrally resolved radiation at the exit slit was detected with a photomultiplier tube after conversion to visible light, centered around 425 nm, by a sodium salicylate scintillator. For spectroscopic investigations at wavelengths below 105 nm, the MHCD device was mounted directly to the entrance slit of a 0.2 m VUV monochromator (wavelength range 50–250 nm, reciprocal linear dispersion of 4 nm/mm). Helium and neon excimer radiation in the wavelength region 60–90 nm from the MHCD enters the monochromator through a 0.2 mm pinhole between the discharge region and the monochromator, which is differentially pumped to provide a operating pressure in the 10^{-5} Torr range in the detector chamber. The VUV photons are detected by a channel electron multiplier connected to a standard pulse counting system. Time-resolved fluorescence spectra are recorded with a SR400 gated photon counting system controlled by a PC.

IV. RESULTS AND DISCUSSION

A. Excimer formation

1. Xenon and argon

Most of the excimer studies so far have focused on Xe excimer emission, with its second continuum peaking at 172 nm. A xenon spectrum for discharge operation with hollow electrodes of 0.1 mm diameter is shown in Fig. 3.¹² At 40 Torr, the 147 nm Xenon resonance line dominates the emission spectra. There are some indications of the first continuum, which extends from the resonance line towards longer wavelength. The second excimer continuum appears prominently at higher pressures and dominates the emission spectra for pressures above 300 Torr. The excimer emission intensity reaches a maximum at approximately 400 Torr and then decreases slightly with increasing pressure.

Argon excimer radiation has its emission maximum at a wavelength of 128 nm. Ar excimer radiation from MHCD plasmas were observed at a lower efficiency compared to Xe. In addition, the argon excimer emission from a MHCD plasma is much more affected by impurities, primarily by nitrogen and carbon lines (possibly due to erosion of the dielectric spacer) and the atomic oxygen resonance lines, which are almost at the same wavelength where the argon

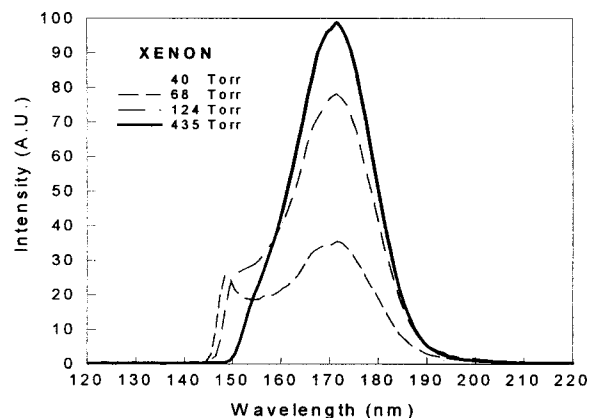


FIG. 3. VUV emission spectra from high-pressure MHCD plasmas in Xe versus gas pressure.

excimer emission has its maximum. Atomic oxygen is generated through collisional dissociation of molecular oxygen, which is present as an impurity. The emission of atomic oxygen triplet lines at 130.2 nm, 130.5 nm, and 130.6 nm from a microhollow cathode discharge in argon with molecular oxygen indicates resonant energy transfer from argon dimers to oxygen atoms (Fig. 4).

2. Argon fluoride and xenon chloride

The generation of high-pressure, direct current discharges in rare gas halide mixtures is more challenging than for rare gases. This is due to instabilities which limit the lifetime of these glow discharges and thus the time of excimer emission to values of the order of 10 ns. However, stable operation up to atmospheric pressure can be achieved by operating rare gas halide discharges in a MHCD geometry. High-pressure discharges in a mixture of 1% F_2 , 5% Ar, and 94% He were found to be intense sources of ArF excimer radiation at 193 nm.⁷ Stable dc operation of MHCDs in a gas mixture containing HCl, another strong attachment, was achieved up to pressures of 1150 Torr.¹⁵ In this mixture, which contained hydrogen chloride (0.06%), xenon (1.5%), and hydrogen (0.03%) and neon as a buffer gas, xenon chloride excimer emission at 308 nm were observed (Fig. 5).

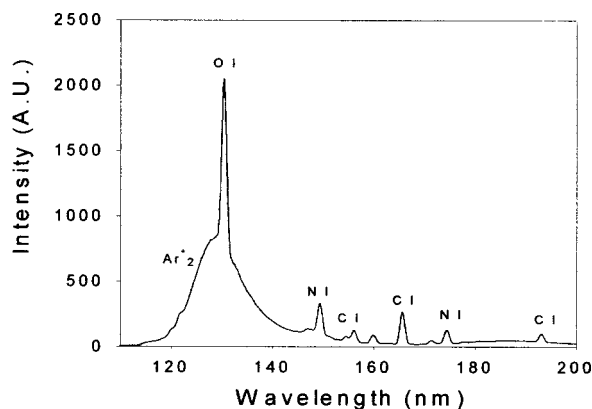


FIG. 4. VUV spectrum of a MHCD plasma in Ar at 850 Torr.

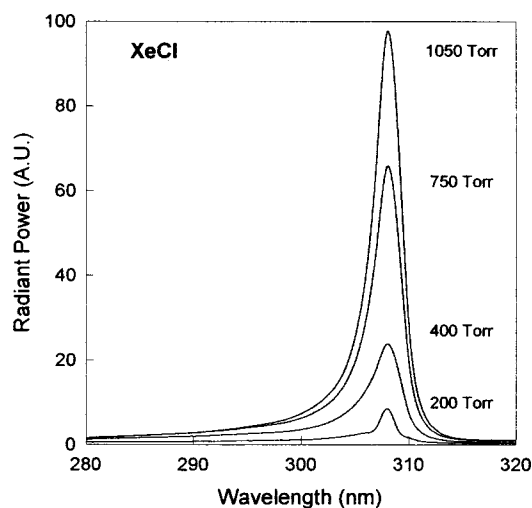


FIG. 5. MHCD xenon chloride excimer spectrum versus gas pressure.

3. Neon and helium

Helium has the widest energy gap between its ground state and the first excited-state manifold (about 20 eV) and the highest ionization energy of all atoms (>24 eV).¹⁶ Nonetheless, He excimer emissions from MHCD plasmas at pressures from 400–600 Torr can readily be obtained.¹⁰ Figure 6 shows the He_2^* excimer emission from a 600 Torr MHCD plasma in pure He. The narrow, sharply peaked feature in the 60–64 nm range corresponds to the first He_2^* excimer continuum and the broad feature extending from 64 nm to almost 100 nm corresponds to the second He_2^* excimer continuum. The small peak in the emission spectrum at about 58 nm is attributed to the He resonance lines whose intensity is drastically reduced due to radiation trapping at these pressures.

Figure 7 (top diagram) shows the Ne excimer emissions from a 740 Torr MHCD plasma in Ne. The narrow emission feature around 75 nm and the broad emission from 78 nm to almost 90 nm are readily identified as, respectively, the first and second Ne_2^* continuum. When a trace amount of H_2 is added to the gas mixture, the emission spectrum changes dramatically and is dominated by the atomic H Lyman- α

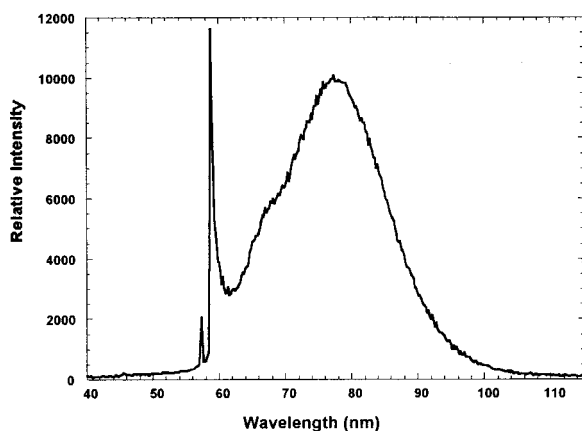


FIG. 6. He_2^* excimer emissions from a 400 Torr MHCD plasma in pure He in the wavelength range 50–100 nm.

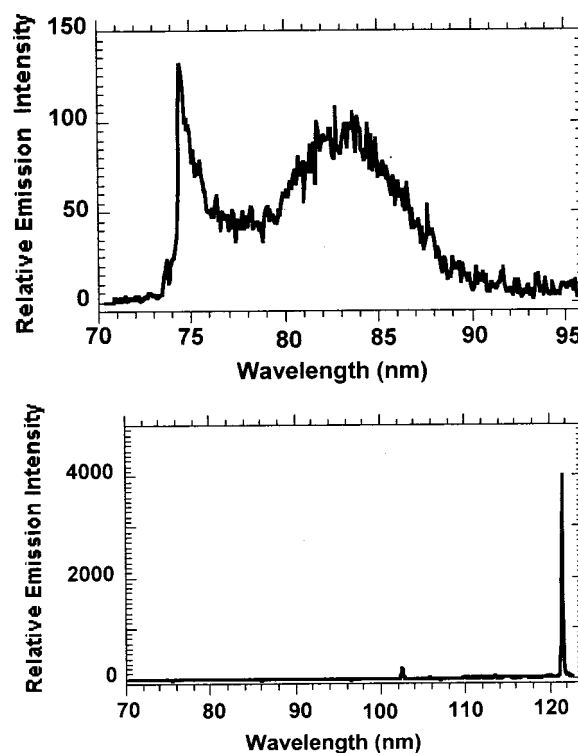


FIG. 7. Top: Ne_2^* excimer emission from a MHCD plasma in pure Ne at 740 Torr in the wavelength range 70–95 nm; bottom: emissions in the 70–125 nm range from a MHCD plasma in 740 Torr Ne with a 0.1% H_2 admixture.

emission at 121.6 nm (Fig. 7, bottom figure). Wieser *et al.*¹⁴ had observed a similar emission of intense, monochromatic H Lyman- α radiation from high-pressure gas mixtures of Ne with trace amounts of H_2 bombarded by high energy electrons and ions and first suggested the above near-resonant energy transfer process as the most likely mechanism leading to the emission of the H Lyman- α line on the basis of spectroscopic studies of the Lyman- α emission. They argued that the Ne_2^* excimers in the bound $^3\Sigma_u$ state have enough energy to dissociate H_2 and excite one of the H atoms to the excited $n=2$ state. The subsequent decay of the excited H atom results in the emission of the 121.6 nm H Lyman- α line. The observation by Kurunczi *et al.*¹⁰ that the Ne_2^* excimer emission essentially disappears as the intense H Lyman- α emission appears in the spectrum provided direct experimental evidence that the near-resonant energy transfer reaction suggested by Wieser *et al.*¹⁴ is indeed the source of the observed intense atomic H emission.

B. Hydrogen Lyman- α emission from MHCD plasmas in high-pressure Ne- H_2 mixtures

The intense H Lyman- α line emission from high-pressure MHCD plasmas in Ne- H_2 mixtures is essentially free of any molecular H_2 background emissions (e.g., the H_2 Werner band emissions) which are characteristic emission features in the wavelength range of the Lyman- α line in spectra obtained from conventional H_2 -containing discharge plasmas of comparable H_2 concentration. The intensity of the observed Lyman- α emission from MHCD plasmas in Ne- H_2 mixtures is orders of magnitude higher than what is observed

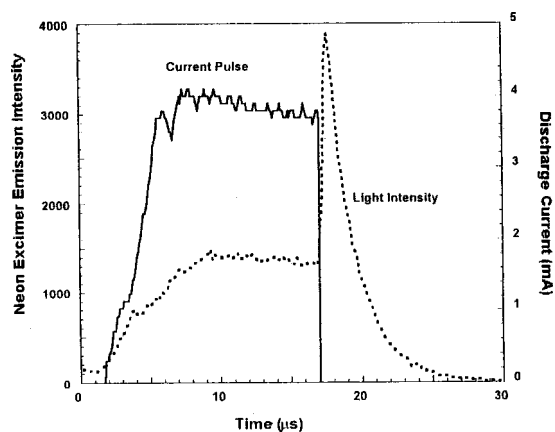


FIG. 8. Time dependence of the current pulse (solid line) and Ne_2^* excimer emission (dashed line) following pulsed dc excitation of a MHCD plasma in Ne at 420 Torr.

in emission spectra from conventional H_2 -containing discharge plasmas of comparable H_2 concentration. This indicates that the rate constant for the near-resonant energy transfer process is much larger than the rate constant corresponding to electron impact dissociative excitation of H_2 leading to the formation of H ($n=2$) atoms by the plasma electrons. In order to determine the rate constant for the near-resonant energy transfer reaction, we carried out a series of time-resolved emission spectroscopic studies of the Ne_2^* excimer emission from pulsed MHCD plasmas in Ne- H_2 mixtures of varying H_2 concentration. The rate equation describing the formation and destruction of $\text{Ne}_2^*(^3\Sigma_u)$ excimers which give rise to the emission of the second continuum following pulsed excitation has the form

$$d[\text{Ne}_2^*]/dt = -[\text{Ne}_2^*] \cdot (A_{ik} + k_q[Q] + k_t[\text{H}_2]), \quad (3)$$

where $[\text{Ne}_2^*]$ and $[\text{H}_2]$ are the densities of the Ne_2^* excimers and the H_2 molecules, respectively, A_{ik} is the inverse of the spontaneous emission lifetime of the $\text{Ne}_2^*(^3\Sigma_u)$ excimer molecules [which has a value of $(8.9)^{-1} \mu\text{s}^{-1}$],¹⁷ $k_q[Q]$ is the sum of all quenching rates, and k_t is the energy transfer rate which we would like to determine. Equation (3) results in an exponential decay of the Ne_2^* light intensity with a decay constant $1/\tau$ given by

$$1/\tau = A_{ik} + 1/k_q[Q] + 1/k_t[\text{H}_2]. \quad (4)$$

A graph of $1/\tau$ versus the H_2 intensity (Stern-Vollmer plot) yields a straight line whose slope allows the determination of the rate constant k_t .

Figure 8 shows the time-resolved emission of the Ne_2^* excimer from a MHCD plasma in 420 Torr Ne following pulsed dc excitation (dashed line). The diagram also depicts the discharge current pulse (solid line) that ignites the MHCD plasma. The point $t=0$ in Fig. 8 was chosen arbitrarily in a way that the figure conveniently displays the entire timing sequence of the experiment. As the discharge current rises to its maximum value of about 4 mA on a time scale of $5 \mu\text{s}$, the excimer emission slowly increases and reaches a steady-state intensity after about $8 \mu\text{s}$ indicating that the excimer formation increases with increasing dis-

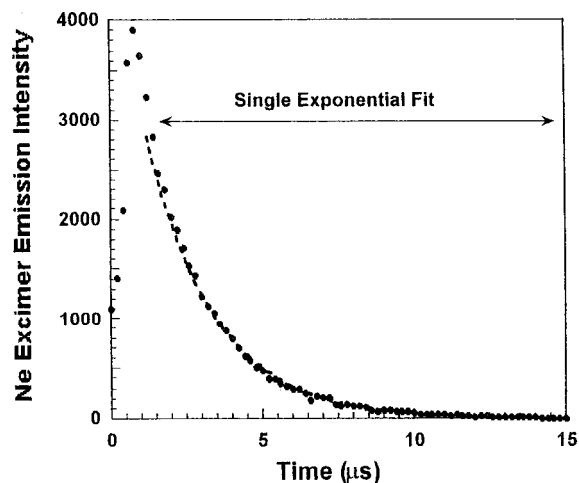


FIG. 9. Time dependence Ne_2^* excimer emission following pulsed dc excitation of a MHCD plasma in Ne at 420 Torr. The time $t=0$ corresponds to the end of the exciting dc current pulse. The dashed line represents a single-exponential fit to the decaying part of the recorded time-resolved emission spectrum.

charge current, as one would expect. After both the discharge current and the excimer emission intensity reach their steady-state values, the current pulse is turned off. Almost immediately, the excimer emission intensity begins to rise sharply and reaches a peak value that is about a factor of 3 higher than the steady-state value during the time the current pulse was applied. We attribute this increase to a rapid cooling of the plasma electrons as the input power to the MHCD plasma is terminated. As the plasma electrons approach zero energy, the recombination step 1(c), which has a sharply peaked cross sections at electron energies close to zero energy and is usually the “bottleneck” in the ionization route becomes temporarily a very efficient channel for excimer formation. Thus, the increase in the excimer formation when the exciting current is terminated can be attributed to a temporary enhancement in the ionization route to excimer formation. Eventually, all excimer formation processes cease and the excimer emission decays exponentially, as one would expect. This is shown in more detail in Fig. 9 in which we labeled the point $t=0$ to coincide with the trailing edge of the exciting current pulse. The rapid rise of the recorded emission intensity is followed by a decay that is well-represented by a single-exponential fit. We obtain a decay constant of the Ne_2^* excimer emission which corresponds to an apparent lifetime of about $2.2 \mu\text{s}$, which is shorter than the natural lifetime of the $\text{Ne}_2^*(^3\Sigma_u)$ excimer state by more than a factor 3. This indicates that quenching processes are very important in MHCD plasma under these operating conditions and, in fact, represent the dominant channel of Ne_2^* excimer destruction.

Figure 10 shows a plot of the inverse decay constants obtained from the single-exponential fit to the measured Ne excimer emissions spectra versus the H_2 concentration obtained from a series of time-resolved spectroscopic studies of pulsed MHCD plasmas in Ne- H_2 mixtures for different H_2 concentrations. It can be seen that the data points are well represented by a straight line. From the slope of the straight

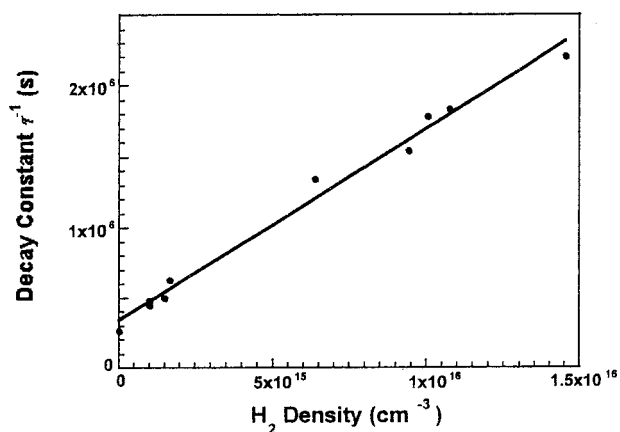


FIG. 10. Plot of the inverse decay time versus the H₂ concentration.

line we obtain a rate constant of about $k_t = 13 \times 10^{-11} \text{ cm}^3/\text{s}$. This value is about four times higher than the value determined indirectly by Wieser *et al.*¹⁴ from their analysis of the time-resolved H Lyman- α emission. We attribute this discrepancy to 2 factors: (i) a higher gas temperature of the MHCD plasma in our case and (ii) the fact that their analysis of the H Lyman- α emission suffered from the re-absorption (radiation trapping) of the Lyman- α photons which leads to an apparently longer decay time and thus a smaller decay constant and a smaller rate constant.¹⁸

V. SUMMARY

Microhollow cathode discharges (MHCDs) are direct current high-pressure gas discharges between a hollow cathode and a planar or hollow anode with hole dimensions in the 0.1–0.5 mm range. The large concentration of high-energy electrons in these discharges, in combination with the high neutral gas density favors three-body processes such as excimer formation. Excimer emission in dc MHCDs in Xe has been observed at an efficiency between 6% and 9%. Other rare gas excimers which have been studied are argon (128 nm), neon (84 nm), and helium (76 nm). Efficiencies are less than for xenon, but still on the order of one percent. In addition near-resonant energy transfer processes in noble gases containing trace amounts of molecular gases, such as

hydrogen and oxygen, have allowed us to use MHCDs as sources of intense line emission at 121.6 nm (H Lyman- α line) and the oxygen triplet between 130.2 and 130.6 nm. Stable dc glow discharges at atmospheric pressure have also been obtained in rare gas/halogen mixtures, providing sources of argon fluoride (193 nm) and xenon chloride (308 nm) excimer radiation. Efficiencies of several percent were measured for argon fluoride and xenon chloride excimer emission. The efficiency can be increased by operating the discharge in a pulsed mode, with nanosecond pulse duration.

ACKNOWLEDGMENTS

This work was supported by the National Science Foundation (NSF), Department of Energy (DOE), and by DARPA/ARO. We also acknowledge financial support from an ARO DURIP equipment award.

- ¹A. El-Habachi and K. H. Schoenbach, *Appl. Phys. Lett.* **72**, 22 (1998).
- ²K. H. Schoenbach, A. El-Habachi, W. Shi, and M. Ciocca, *Plasma Sources Sci. Technol.* **6**, 468 (1997).
- ³A. Güntherschulze, *Z. Tech. Phys. (Leipzig)* **19**, 49 (1923).
- ⁴A. Walsh, *Spectrochim. Acta* **7**, 108 (1956).
- ⁵H. Helm, *Z. Naturforsch.* **27a**, 1712 (1972).
- ⁶G. Stockhausen and M. Kock, *J. Phys. D* **34**, 1683 (2001).
- ⁷K. H. Schoenbach, A. El-Habachi, M. M. Moselhy, W. Shi, and R. H. Stark, *Phys. Plasmas* **7**, 2186 (2000).
- ⁸A. El-Habachi and K. H. Schoenbach, *Appl. Phys. Lett.* **72**, 22 (1998).
- ⁹M. Moselhy, A. El-Habachi, K. H. Schoenbach, and U. Kogelschatz, *Appl. Phys. Lett.* **78**, 880 (2001).
- ¹⁰P. Kurunczi, H. Shah, and K. Becker, *J. Phys. B* **32**, L651 (1999).
- ¹¹P. Kurunczi, J. Lopez, H. Shah, and K. Becker, *Int. J. Mass. Spectrom.* **205**, 277 (2001).
- ¹²W. Waller, U. Schaller, and H. Langhoff, *J. Chem. Phys.* **83**, 1667 (1985).
- ¹³D. C. Lorents, *Physica C* **82**, 19 (1976).
- ¹⁴J. Wieser, M. Salvermoser, L. H. Shah, A. Ulrich, D. E. Murnick, and H. Dahl, *J. Phys. B* **31**, 4589 (1998).
- ¹⁵A. El-Habachi, W. Shi, M. M. Moselhy, R. H. Stark, and K. H. Schoenbach, *J. Appl. Phys.* **88**, 3220 (2000).
- ¹⁶I. I. Sobelman, *Atomic Spectra and Radiative Transitions*, Springer Series in Chemical Physics (Springer-Verlag, Berlin, 1979), Vol. 1.
- ¹⁷See, e.g., M. McCusker, "The rare gas excimers," in *Excimer Lasers*, edited by C. K. Rhodes (Springer-Verlag, Heidelberg, 1984) and references therein to earlier publications; as discussed in this article, the radiative lifetime of the Ne₂^{*}(³Σ_u) excimer state has been measured by several authors who report values ranging from 5.1 μs to 12 μs with an average value of 8.9 μs which has an estimated uncertainty of no less than about 30%.
- ¹⁸M. Salvermoser (private communication, 2001).